Some unconditionally stable time stepping methods for the 3-D Maxwell's equations

Jongwoo Lee [a,1,*], Bengt Fornberg [b,2]

[a]*Kwangwoon University, Department of Mathematics, 447-1 Wolgye-Dong, Nowon-Gu, Seoul 139-701, Korea*

[b]*University of Colorado, Department of Applied Mathematics, 526 UCB, Boulder, CO 80309, USA*

Abstract

Almost all the difficulties that arise in the numerical solution of Maxwell's equations are due to material interfaces. In case that their geometrical features are much smaller than a typical wave length, one would like to use small space steps with large time steps. The first time stepping method which combines a very low cost per time step with unconditional stability was the ADI-FDTD method introduced in 1999. The present discussion starts with this method, and with an even more recent Crank-Nicolson-based split step method with similar properties. We then explore how these methods can be made even more efficient by combining them with techniques that increase their temporal accuracies.

Key words: Maxwell's equations, ADI-FDTD, Crank-Nicolson, split step, Richardson extrapolation, Deferred correction
2000 MSC: 65M70, 65M06, 78M2

1 Introduction

There are two different length scales present in CEM (computational electromagnetics) problems:

- The size of geometrical features, and
- A typical wave length.

In many problems, the two length scales are of comparable size. The (partly conflicting) goals that then need to be met by an effective numerical method include

- Good geometric flexibility (to allow for interfaces with corners or with high curvatures),
- High order of spatial accuracy (to keep the number of points per wavelength low),
- Guaranteed (conditional) time stepping stability,
- Low computational cost.

There are also many important applications in which the first length scale (the size of geometrical features) is far smaller than a typical wave length - maybe by five orders of magnitude, or more. Examples of such situations include

- Modeling of a computer chip operating around 1 GHz. In this case the wave length is about $30\,\text{cm}$ and typical distance between components is about $1\,\mu\text{m}$, so the ratio between the two length scales is more than 3×10^5,
- Lightning strike on aircraft. Frequency of lightning wave is around 10 KHz (wave length about $30\,\text{km}$) and width of a typical airplane window is around $30\,\text{cm}$. So the ratio between two length scales is about 1×10^5, and
- Effect of microwaves on brain cells. The ratio between two length scales is also about same numbers as above.

In order to capture the geometry, we then need to use grids with an extremely high number of points per wavelength (PPW). High formal order of accuracy in the spatial discretization is therefore less critical. On the other hand, the method to advance in time should now feature

- Explicit (or effectively explicit) time stepping (since grids tend to be extremely large), and
- Complete absence of any CFL-type stability conditions (since such conditions would force time step sizes many orders of magnitude smaller than what is needed in order to accurately resolve the wave).

The first method that met both of these criteria was introduced by Zheng et al. in 1999 [23]. Since then, another (partly related) method has been proposed by [9]. With the latter method implemented using a Crank-Nicolson split step (CNS) discretization, both of the approaches require, as their only nontrivial step, the solution of tridiagonal linear systems.

In this article, we will first state the 3-D Maxwell's equations formulated in 1873 by James Clark Maxwell [11], and then summarize the classical Yee

scheme [21]. Following that, we will introduce the ADI and CNS schemes. After that, we present three different approaches to enhance the temporal accuracy of these natively second order schemes, and we compare the resulting computational efficiencies.

For two of the three approaches - extrapolation and deferred correction - unconditional stability is preserved for all orders, as long as this holds for the underlying second order ADI and CNS schemes (proven for initial value problems, but seems to be true also in the presence of general boundary conditions). Regarding the third approach - special time step sequences - the fourth order version appears to be unconditionally stable, but no proof has yet been found.

In Section 7, we present numerical experiments which feature interfaces and boundaries, and find that the time stepping situation has not become adversely affected. We conclude with some remarks about possible future directions of study.

2 Maxwell's equations, and the Yee scheme

For a medium with permittivity ε and permeability μ, assuming no free charges or currents, the 3-D Maxwell's equations can be written

$$
\begin{cases}
\dfrac{\partial E_x}{\partial t} &= \dfrac{1}{\varepsilon}\left(\dfrac{\partial H_z}{\partial y} - \dfrac{\partial H_y}{\partial z}\right) \\[2mm]
\dfrac{\partial E_y}{\partial t} &= \dfrac{1}{\varepsilon}\left(\dfrac{\partial H_x}{\partial z} - \dfrac{\partial H_z}{\partial x}\right) \\[2mm]
\dfrac{\partial E_z}{\partial t} &= \dfrac{1}{\varepsilon}\left(\dfrac{\partial H_y}{\partial x} - \dfrac{\partial H_x}{\partial y}\right) \\[2mm]
\dfrac{\partial H_x}{\partial t} = -\dfrac{1}{\mu}\left(\dfrac{\partial E_z}{\partial y} - \dfrac{\partial E_y}{\partial z}\right) \\[2mm]
\dfrac{\partial H_y}{\partial t} = -\dfrac{1}{\mu}\left(\dfrac{\partial E_x}{\partial z} - \dfrac{\partial E_z}{\partial x}\right) \\[2mm]
\dfrac{\partial H_z}{\partial t} = -\dfrac{1}{\mu}\left(\dfrac{\partial E_y}{\partial x} - \dfrac{\partial E_x}{\partial y}\right)
\end{cases} ,
\tag{2.1}
$$

where E_x, E_y, E_z and H_x, H_y, H_z denote the components of the electric filed $\mathbf{E}$ and magnetic field $\mathbf{H}$. If these fields (multiplied with ε and μ respectively) start out divergence free, they will remain so during wave propagation. Physically this is a consequence of the relations $\mathrm{div}(\varepsilon\mathbf{E}) = \rho$ (where ρ is the local charge density), and $\mathrm{div}(\mu\mathbf{H}) = 0$. Their invariance in time is also a consequence of

(2.1) and need therefore not be imposed separately:

$$\frac{\partial}{\partial t}\left(\operatorname{div}\varepsilon\mathbf{E}\right) = \frac{\partial}{\partial t}\left(\frac{\partial\varepsilon E_x}{\partial x} + \frac{\partial\varepsilon E_y}{\partial y} + \frac{\partial\varepsilon E_z}{\partial z}\right)$$

$$= \frac{\partial}{\partial x}\left(\frac{\partial H_z}{\partial y} - \frac{\partial H_y}{\partial z}\right) + \frac{\partial}{\partial y}\left(\frac{\partial H_x}{\partial z} - \frac{\partial H_z}{\partial x}\right) + \frac{\partial}{\partial z}\left(\frac{\partial H_y}{\partial x} - \frac{\partial H_x}{\partial y}\right) \quad (2.2)$$

$$= 0$$

and similarly for $\operatorname{div}(\mu\mathbf{H})$.

Arguably, the simplest possible finite difference approximation to (2.1) consists of approximating each derivative (in space and time) by centered second order finite differences, i.e.

$$(2.3)$$

$$\begin{cases}
\dfrac{E_x|_{i,j,k}^{n+1} - E_x|_{i,j,k}^{n-1}}{2\Delta t} = \dfrac{1}{\varepsilon}\left(\dfrac{H_z|_{i,j+1,k}^{n} - H_z|_{i,j-1,k}^{n}}{2\Delta y} - \dfrac{H_y|_{i,j,k+1}^{n} - H_y|_{i,j,k-1}^{n}}{2\Delta z}\right) \\[2ex]
\dfrac{E_y|_{i,j,k}^{n+1} - E_y|_{i,j,k}^{n-1}}{2\Delta t} = \dfrac{1}{\varepsilon}\left(\dfrac{H_x|_{i,j,k+1}^{n} - H_x|_{i,j,k-1}^{n}}{2\Delta z} - \dfrac{H_z|_{i+1,j,k}^{n} - H_z|_{i-1,j,k}^{n}}{2\Delta x}\right) \\[2ex]
\dfrac{E_z|_{i,j,k}^{n+1} - E_z|_{i,j,k}^{n-1}}{2\Delta t} = \dfrac{1}{\varepsilon}\left(\dfrac{H_y|_{i+1,j,k}^{n} - H_y|_{i-1,j,k}^{n}}{2\Delta x} - \dfrac{H_x|_{i,j+1,k}^{n} - H_x|_{i,j-1,k}^{n}}{2\Delta y}\right) \\[2ex]
\dfrac{H_x|_{i,j,k}^{n+1} - H_x|_{i,j,k}^{n-1}}{2\Delta t} = -\dfrac{1}{\mu}\left(\dfrac{E_z|_{i,j+1,k}^{n} - E_z|_{i,j-1,k}^{n}}{2\Delta y} - \dfrac{E_y|_{i,j,k+1}^{n} - E_y|_{i,j,k-1}^{n}}{2\Delta z}\right) \\[2ex]
\dfrac{H_y|_{i,j,k}^{n+1} - H_y|_{i,j,k}^{n-1}}{2\Delta t} = -\dfrac{1}{\mu}\left(\dfrac{E_x|_{i,j,k+1}^{n} - E_x|_{i,j,k-1}^{n}}{2\Delta z} - \dfrac{E_z|_{i+1,j,k}^{n} - E_z|_{i-1,j,k}^{n}}{2\Delta x}\right) \\[2ex]
\dfrac{H_z|_{i,j,k}^{n+1} - H_z|_{i,j,k}^{n-1}}{2\Delta t} = -\dfrac{1}{\mu}\left(\dfrac{E_y|_{i+1,j,k}^{n} - E_y|_{i-1,j,k}^{n}}{2\Delta x} - \dfrac{E_x|_{i,j+1,k}^{n} - E_x|_{i,j-1,k}^{n}}{2\Delta y}\right)
\end{cases}$$

In the style of (2.2), we can see that (2.3) exactly preserves discrete analogs of $\operatorname{div}(\varepsilon\mathbf{E})$ and $\operatorname{div}(\mu\mathbf{H})$.

Another key to the long-standing popularity of this Yee scheme [21,19,8] is the concept of grid staggering. Representing each of our six unknowns at every (Cartesian) grid point leads effectively to 16 entirely uncoupled computations. For one such computation, each variable needs only be present at one out of every 8 node points, and furthermore, only at every second time level.

The lack of geometrical constraints in the time direction makes it particularly easy to use high order (big stencil) methods in that direction. The main reason this is not routinely utilized has to do with stability. For the Yee scheme, it can be shown (for example by von Neumann analysis) that computations will be unstable unless $\Delta t < 1\,/\,(c\,\sqrt{1/(\Delta x)^2 + 1/(\Delta y)^2 + 1/(\Delta z)^2}\,)$, where $c = 1/\sqrt{\varepsilon\mu}$ is the wave speed. In this case, the actual stability constraint agrees exactly with the (often not sharp) upper bound on the time step imposed by the CFL (Courant-Friedrichs-Levy) condition. This condition usually makes it pointless to try to use higher order accuracy in time than what is used in space.

Although doing so would increase the temporal accuracy, stability constraints would prevent this from being utilized to gain computational efficiency through the use of significantly larger time steps.

3 Two second order and unconditionally stable methods

In cases with extremely fine geometrical features, it may be necessary to compute with thousands of points per wave length (PPW). The Yee scheme's CFL stability condition would then require extremely short time steps (compared to what is needed for accuracy). We will next describe two approaches that are computationally fast, but still avoid the CFL restriction. They permit time steps to be chosen based on accuracy- and not stability considerations.

3.1 Alternating direction implicit method (ADI) - original description

The ADI approach has been used very successfully for parabolic and elliptic PDEs since about 50 years ago. Seminal papers in the area include for ex. [14] and [2]. Similar 3-stage dimensional splittings for the 3-D Maxwell's equations have been repeatedly tried in various forms since then, but have invariably fallen short of the goal of unconditional time stability. However, a 2-stage splitting introduced in 1999 by Zheng et al. [23,24] does achieve the goal. The original way to state this scheme includes introducing a half-way time level $n + 1/2$ between the adjacent time levels n and $n + 1$. We advance our six variables as follows:

Stage 1:

$$
\begin{cases}
\dfrac{E_x|_{i,j,k}^{n+\frac{1}{2}} - E_x|_{i,j,k}^{n}}{\Delta t/2} = \dfrac{1}{\varepsilon}\left(\dfrac{H_z|_{i,j+1,k}^{n+\frac{1}{2}} - H_z|_{i,j-1,k}^{n+\frac{1}{2}}}{2\Delta y} - \dfrac{H_y|_{i,j,k+1}^{n} - H_y|_{i,j,k-1}^{n}}{2\Delta z}\right) \\[3ex]
\dfrac{E_y|_{i,j,k}^{n+\frac{1}{2}} - E_y|_{i,j,k}^{n}}{\Delta t/2} = \dfrac{1}{\varepsilon}\left(\dfrac{H_x|_{i,j,k+1}^{n+\frac{1}{2}} - H_x|_{i,j,k-1}^{n+\frac{1}{2}}}{2\Delta z} - \dfrac{H_z|_{i+1,j,k}^{n} - H_z|_{i-1,j,k}^{n}}{2\Delta x}\right) \\[3ex]
\dfrac{E_z|_{i,j,k}^{n+\frac{1}{2}} - E_z|_{i,j,k}^{n}}{\Delta t/2} = \dfrac{1}{\varepsilon}\left(\dfrac{H_y|_{i+1,j,k}^{n+\frac{1}{2}} - H_y|_{i-1,j,k}^{n+\frac{1}{2}}}{2\Delta x} - \dfrac{H_x|_{i,j+1,k}^{n} - H_x|_{i,j-1,k}^{n}}{2\Delta y}\right) \\[3ex]
\dfrac{H_x|_{i,j,k}^{n+\frac{1}{2}} - H_x|_{i,j,k}^{n}}{\Delta t/2} = \dfrac{1}{\mu}\left(\dfrac{E_y|_{i,j,k+1}^{n+\frac{1}{2}} - E_y|_{i,j,k-1}^{n+\frac{1}{2}}}{2\Delta z} - \dfrac{E_z|_{i,j+1,k}^{n} - E_z|_{i,j-1,k}^{n}}{2\Delta y}\right) \\[3ex]
\dfrac{H_y|_{i,j,k}^{n+\frac{1}{2}} - H_y|_{i,j,k}^{n}}{\Delta t/2} = \dfrac{1}{\mu}\left(\dfrac{E_z|_{i+1,j,k}^{n+\frac{1}{2}} - E_z|_{i-1,j,k}^{n+\frac{1}{2}}}{2\Delta x} - \dfrac{E_x|_{i,j,k+1}^{n} - E_x|_{i,j,k-1}^{n}}{2\Delta z}\right) \\[3ex]
\dfrac{H_z|_{i,j,k}^{n+\frac{1}{2}} - H_z|_{i,j,k}^{n}}{\Delta t/2} = \dfrac{1}{\mu}\left(\dfrac{E_x|_{i,j+1,k}^{n+\frac{1}{2}} - E_x|_{i,j-1,k}^{n+\frac{1}{2}}}{2\Delta y} - \dfrac{E_y|_{i+1,j,k}^{n} - E_y|_{i-1,j,k}^{n}}{2\Delta x}\right)
\end{cases}
\tag{3.1}
$$

Stage 2:

$$
\begin{cases}
\dfrac{E_x|_{i,j,k}^{n+1} - E_x|_{i,j,k}^{n+\frac{1}{2}}}{\Delta t/2} = \dfrac{1}{\varepsilon}\left(\dfrac{H_z|_{i,j+1,k}^{n+\frac{1}{2}} - H_z|_{i,j-1,k}^{n+\frac{1}{2}}}{2\Delta y} - \dfrac{H_y|_{i,j,k+1}^{n+1} - H_y|_{i,j,k-1}^{n+1}}{2\Delta z} \right) \\[2.2em]
\dfrac{E_y|_{i,j,k}^{n+1} - E_y|_{i,j,k}^{n+\frac{1}{2}}}{\Delta t/2} = \dfrac{1}{\varepsilon}\left(\dfrac{H_x|_{i,j,k+1}^{n+\frac{1}{2}} - H_x|_{i,j,k-1}^{n+\frac{1}{2}}}{2\Delta z} - \dfrac{H_z|_{i+1,j,k}^{n+1} - H_z|_{i-1,j,k}^{n+1}}{2\Delta x} \right) \\[2.2em]
\dfrac{E_z|_{i,j,k}^{n+1} - E_z|_{i,j,k}^{n+\frac{1}{2}}}{\Delta t/2} = \dfrac{1}{\varepsilon}\left(\dfrac{H_y|_{i+1,j,k}^{n+\frac{1}{2}} - H_y|_{i-1,j,k}^{n+\frac{1}{2}}}{2\Delta x} - \dfrac{H_x|_{i,j+1,k}^{n+1} - H_x|_{i,j-1,k}^{n+1}}{2\Delta y} \right) \\[2.2em]
\dfrac{H_x|_{i,j,k}^{n+1} - H_x|_{i,j,k}^{n+\frac{1}{2}}}{\Delta t/2} = \dfrac{1}{\mu}\left(\dfrac{E_y|_{i,j,k+1}^{n+\frac{1}{2}} - E_y|_{i,j,k-1}^{n+\frac{1}{2}}}{2\Delta z} - \dfrac{E_z|_{i,j+1,k}^{n+1} - E_z|_{i,j-1,k}^{n+1}}{2\Delta y} \right) \\[2.2em]
\dfrac{H_y|_{i,j,k}^{n+1} - H_y|_{i,j,k}^{n+\frac{1}{2}}}{\Delta t/2} = \dfrac{1}{\mu}\left(\dfrac{E_z|_{i+1,j,k}^{n+\frac{1}{2}} - E_z|_{i-1,j,k}^{n+\frac{1}{2}}}{2\Delta x} - \dfrac{E_x|_{i,j,k+1}^{n+1} - E_x|_{i,j,k-1}^{n+1}}{2\Delta z} \right) \\[2.2em]
\dfrac{H_z|_{i,j,k}^{n+1} - H_z|_{i,j,k}^{n+\frac{1}{2}}}{\Delta t/2} = \dfrac{1}{\mu}\left(\dfrac{E_x|_{i,j+1,k}^{n+\frac{1}{2}} - E_x|_{i,j-1,k}^{n+\frac{1}{2}}}{2\Delta y} - \dfrac{E_y|_{i+1,j,k}^{n+1} - E_y|_{i-1,j,k}^{n+1}}{2\Delta x} \right)
\end{cases}
\tag{3.2}
$$

Several things can be noted:

- The stages differ in that we swap which of the two terms in each right hand side (RHS) that is discretized on the new and which on the old time level.
- On each new time level, we can obtain tridiagonal linear systems for E_x, E_y, E_z. For ex. in Stage 1, on the new time level, we can eliminate H_z between the first and the last equation, giving a tridiagonal system for E_x. Once we similarly get (and solve) the tridiagonal systems also for E_y and E_z, the remaining variables H_x, H_y, H_z follow explicitly
- Yee-type staggering can again be applied, but only in space, giving savings by a factor of 8 compared to the case when all variables are represented at all grid points.
- The solution at the intermediate time level $n + 1/2$ is only first order accurate. However, the accuracy is second order after each completed pair of stages (i.e. at all integer-numbered time levels).

Shortly after this ADI scheme was first proposed, Namiki [12] demonstrated its practical advantages for two test problems (a monopole antenna near a thin dielectric wall, and a stripline with a narrow gap). This scheme has also, by Liu and Gedney [10], been found to work well together with PML far field boundary conditions.

3.1.1 Proofs of unconditional stability

The original proof of unconditional stability, given in [24], uses von Neumann analysis. This leads to the demanding task of analytically determining the eigenvalues of a certain 6×6 matrix, whose entries are functions of the grid steps and wave numbers. This turns out to be feasible, but only through some quite heavy use computational symbolic algebra. It transpires that all the

eigenvalues have magnitude one, which establishes the unconditional stability. A much simpler energy-based stability proof was given by Fornberg [3,4]. Considering (3.1) and (3.2) on a periodic cube with arbitrary grid spacings in the three dimensions, it follows, after just a few lines of algebraic manipulations, that the expression

$$\sum_{i,j,k} \left\{ \varepsilon \left\{ \left(E_x|_{i,j,k}^n \right)^2 + \left(E_y|_{i,j,k}^n \right)^2 + \left(E_z|_{i,j,k}^n \right)^2 \right\} + \mu \left\{ \left(H_x|_{i,j,k}^n \right)^2 + \left(H_y|_{i,j,k}^n \right)^2 + \left(H_z|_{i,j,k}^n \right)^2 \right\} \right\}$$

(with the sum running over all the grid points) remains bounded for all times. This rules out any possibility of growing Fourier modes. Although it has not been exploited yet in this case, such 'energy-type' proofs often allow extensions to cases of variable coefficients (i.e. variable media) and to different types of boundary conditions. A third proof is given in [1]. The matrix which describes how the ADI solution is advanced over the two stages is shown to be similar to a unitary matrix, implying that all its eigenvalues are of magnitude one.

3.2 Alternative description of the ADI method

Maxwell's equations (2.1) can be written

$$\frac{\partial}{\partial t} \begin{bmatrix} E_x \\ E_y \\ E_z \\ H_x \\ H_y \\ H_z \end{bmatrix} = \begin{bmatrix} \dfrac{1}{\varepsilon}\dfrac{\partial H_z}{\partial y} \\ \dfrac{1}{\varepsilon}\dfrac{\partial H_x}{\partial z} \\ \dfrac{1}{\varepsilon}\dfrac{\partial H_y}{\partial x} \\ \dfrac{1}{\mu}\dfrac{\partial E_y}{\partial z} \\ \dfrac{1}{\mu}\dfrac{\partial E_z}{\partial x} \\ \dfrac{1}{\mu}\dfrac{\partial E_x}{\partial y} \end{bmatrix} + \begin{bmatrix} -\dfrac{1}{\varepsilon}\dfrac{\partial H_y}{\partial z} \\ -\dfrac{1}{\varepsilon}\dfrac{\partial H_z}{\partial x} \\ -\dfrac{1}{\varepsilon}\dfrac{\partial H_x}{\partial y} \\ -\dfrac{1}{\mu}\dfrac{\partial E_z}{\partial y} \\ -\dfrac{1}{\mu}\dfrac{\partial E_x}{\partial z} \\ -\dfrac{1}{\mu}\dfrac{\partial E_y}{\partial x} \end{bmatrix} \tag{3.3}$$

or, more briefly,

$$\frac{\partial \underline{u}}{\partial t} = A\,\underline{u} + B\,\underline{u}\,.$$

The standard Crank-Nicolson approximation becomes

$$\frac{\underline{u}^{n+1} - \underline{u}^n}{\Delta t} = \frac{1}{2}(A\underline{u}^{n+1} + A\underline{u}^n) + \frac{1}{2}(B\underline{u}^{n+1} + B\underline{u}^n) + O(\Delta t)^2$$

7

$$\Rightarrow \left(1 - \frac{\Delta t}{2}A - \frac{\Delta t}{2}B\right)\underline{u}^{n+1} = \left(1 + \frac{\Delta t}{2}A + \frac{\Delta t}{2}B\right)\underline{u}^n + O(\Delta t)^3$$

$$\Rightarrow \underbrace{\left(1 - \frac{\Delta t}{2}A\right)\left(1 - \frac{\Delta t}{2}B\right)\underline{u}^{n+1} = \left(1 + \frac{\Delta t}{2}A\right)\left(1 + \frac{\Delta t}{2}B\right)\underline{u}^n}_{\text{One-step approximation}}$$

$$+ \underbrace{\frac{(\Delta t)^2}{4} A \, B(\underline{u}^{n+1} - \underline{u}^n) + O(\Delta t)^3}_{\text{Error} = O(\Delta t)^3} \tag{3.4}$$

The 'One-step approximation'

$$\left(1 - \frac{\Delta t}{2}A\right)\left(1 - \frac{\Delta t}{2}B\right)\underline{u}^{n+1} = \left(1 + \frac{\Delta t}{2}A\right)\left(1 + \frac{\Delta t}{2}B\right)\underline{u}^n \tag{3.5}$$

can be written in two stages

$$\begin{cases} \left(1 - \frac{\Delta t}{2}A\right)\underline{u}^{n+\frac{1}{2}} = \left(1 + \frac{\Delta t}{2}B\right)\underline{u}^n \\ \left(1 - \frac{\Delta t}{2}B\right)\underline{u}^{n+1} = \left(1 + \frac{\Delta t}{2}A\right)\underline{u}^{n+\frac{1}{2}} \end{cases}. \tag{3.6}$$

To verify this, we multiply the first equation of (3.6) by $\left(1 + \frac{\Delta t}{2}A\right)$ and the second one by $\left(1 - \frac{\Delta t}{2}A\right)$. The LHS of the first equation then equals the RHS of the second equation, and (3.5) follows. It is straightforward to verify that the two equations in (3.6) - after space derivatives in A and B have been replaced by centered finite differences - become equivalent to the two stages (3.1) and (3.2) of the ADI scheme. This way of deriving the ADI method (independently noted also in [1] and [6]) offers us several advantages:

- We recognize that $\underline{u}^{n+1/2}$ more naturally can be seen just as an intermediate computational quantity rather than as some specific intermediate time level (at which we have reduced accuracy).
- The second order accuracy in time for the overall procedure has become obvious.
- It becomes easy to determine the precise form of the local temporal error (which will be of importance to us later for implementing deferred correction in order to reach higher orders of accuracy in time).

3.3 Crank-Nicolson based split-step method (CNS)

We start this subsection by briefly reviewing the general concept and history of split step methods, and we then note how they can be applied to the Maxwell's

equations.

3.3.1 Concept of general split-step methods

In the simplest form of split step, featuring only first order accuracy in time, one would advance an ODE (or a system of ODEs)

$$u_t = A(u) + B(u) \tag{3.7}$$

from time t to time $t + \Delta t$ by successively solving

$$u_t = 2A(u) \quad \text{from} \ \ t \ \ \text{to} \ t + \frac{1}{2}\Delta t, \ \ \text{followed by}$$
$$u_t = 2B(u) \quad \text{from} \ t + \frac{1}{2}\Delta t \ \ \text{to} \ \ t + \Delta t$$

Here, $A(u)$ and $B(u)$ can be very general nonlinear operators (in particular, there is no requirement that A and B commute). The two time increments are each of length $\frac{1}{2}\Delta t$. We therefore denote this splitting by $\left\{\frac{1}{2}, \frac{1}{2}\right\}$. One obtains second-order accuracy in time by instead alternating the two equations in the pattern A, B, A while using the time increments $\left\{\frac{1}{4}, \frac{1}{2}, \frac{1}{4}\right\}$ - known as 'Strang splitting' [17]. In 1990 Yoshida [22] devised a systematic way to obtain similar split step methods of still higher orders. From an implementation standpoint, one simply chooses certain longer time increment sequences, while again alternating A, B, A, B, ... Table 3.1 shows the coefficients of methods of orders 1, 2, 4, 6, and 8. The coefficients for the methods of order 6 and above are not unique. In some applications, the main use of the split-step approach is to separate an ODE that lacks a closed-form solution into a couple of ODEs which both allow such solutions. The approach is however especially interesting for PDEs. If such an equation is of the form $u_t + A(u, u_x) + B(u, u_y) = 0$, immediate dimensional splitting leads to two 1-D problems. Splitting is also of significant interest for certain nonlinear wave equations (see for ex. [5] for comparisons between split step and two other approaches). For example, the Korteweg-de Vries (KdV) equation $u_t + uu_x + u_{xxx} = 0$ can be split into $u_t + 2uu_x = 0$ (which features few numerical difficulties over brief times) and $u_t + 2u_{xxx} = 0$ (which is linear, and can be solved analytically, thereby bypassing otherwise severe stability restrictions).

It can be shown (Suzuki, [18]) that methods of orders above 2 will need to feature at least some negative time increments. Although this is of little concern in our context of Maxwell's equations, it does make the splitting idea problematic in cases when an equation is partly dissipative, such as for example the Navier-Stokes equations.

For a heuristic perspective on higher order split-step methods, we refer to [9]. See also [13] and [22]. The key contributions by Yoshida in 1990 [22] were to

Table 3.1

Coefficients of some Split-Step methods. For details, see [22,9].

METHOD	TIME INCREMENT SEQUENCE		
SS1	0.50000 00000 00000 00000	0.50000 00000 00000 00000	
SS2	0.25000 00000 00000 00000	0.50000 00000 00000 00000	0.25000 00000 00000 00000
SS4	0.33780 17979 89914 40851	0.67560 35959 79828 81702	-0.08780 17979 89914 40851
	-0.85120 71919 59657 63405	-0.08780 17979 89914 40851	0.67560 35959 79828 81702
	0.33780 17979 89914 40851		
SS6	0.19612 84026 19389 31595	0.39225 68052 38778 63191	0.25502 17059 59228 84938
	0.11778 66066 79679 06684	-0.23552 66927 04878 21832	-0.58883 99920 89435 50347
	0.03437 65841 26260 05298	0.65759 31603 41955 60944	0.03437 65841 26260 05298
	-0.58883 99920 89435 50347	-0.23552 66927 04878 21832	0.11778 66066 79679 06684
	0.25502 17059 59228 84938	0.39225 68052 38778 63191	0.19612 84026 19389 31595
SS8	0.22871 10615 57447 89169	0.45742 21231 14895 78337	0.29213 43956 99000 73022
	0.12684 66682 83105 67707	-0.29778 97250 73598 45089	-0.72242 61184 30302 57885
	-0.40077 32180 57163 83322	-0.07912 03176 84025 08760	0.44497 46255 63618 95284
	0.96906 95688 11262 99329	-0.00561 77738 38196 20526	-0.98030 51164 87655 40380
	-0.46445 25958 95878 59173	0.05139 99246 95898 22035	0.45281 32300 44769 50634
	0.85422 65353 93640 79233	0.45281 32300 44769 50634	0.05139 99246 95898 22035
	-0.46445 25958 95878 59173	-0.98030 51164 87655 40380	-0.00561 77738 38196 20526
	0.96906 95688 11262 99329	0.44497 46255 63618 95284	-0.07912 03176 84025 08760
	-0.40077 32180 57163 83322	-0.72242 61184 30302 57885	-0.29778 97250 73598 45089
	0.12684 66682 83105 67707	0.29213 43956 99000 73022	0.45742 21231 14895 78337
	0.22871 10615 57447 89169		

- Demonstrate that it is possible to find sequences of time increments that give time stepping accuracies of any order.
- Device a practical algorithm for computing these sequences of increments.
- Note that, to get a high order in time, special time step sequences can be applied as an addition to any scheme that is second order accurate (i.e. if we have any second order scheme for (3.3) - irrespective of if it is itself based on splitting or not - we can use certain time stepping sequences to bring it up to any order in time).

A couple of comments regarding the last point above:

- We can use either ADI or CNS (Strang splitted 3-D Maxwell's equations, using Crank-Nicolson for the sub-problems - as will be described next) as our basic scheme, and then use special time step sequences to enhance it to higher orders. This will become one of the three enhancement techniques we will consider later for increasing the time accuracy of the unconditionally stable ADI and CNS schemes.
- The methods SS4, SS6, SS8 in Table 3.1 are just special cases of this more general observation. These schemes arise if we choose CNS (also denoted SS2) as our basic second order scheme.

Immediate dimensional splitting of the 3-D Maxwell's equations would lead us to consider a PDE of the form $\frac{\partial \underline{u}}{\partial t} = A\underline{u} + B\underline{u} + C\underline{u}$ where $\underline{u}$ denotes the vector $(E_x, E_y, E_z, H_x, H_y, H_z)^T$. Although 3-way splitting is feasible, the particular structure of the 3-D Maxwell's equations permits a much more effective alternative. We start this by writing the Maxwell's equations as we did earlier in (3.3) and, like then, we abbreviate them as

$$\frac{\partial \underline{u}}{\partial t} = A\underline{u} + B\underline{u}. \tag{3.8}$$

The split-step approach leads us to repeatedly advance $\dfrac{\partial \underline{u}}{\partial t} = 2A\underline{u}$ and $\dfrac{\partial \underline{u}}{\partial t} = 2B\underline{u}$ by certain time increments. These two subproblems can be written out explicitly as shown below. As first noted by Lee and Fornberg [9], each of the subproblems amounts to three pairs of mutually entirely uncoupled 1-D equations:

$$\left\{
\begin{array}{c}
\left\{
\begin{array}{l}
\dfrac{\partial E_x}{\partial t} = \dfrac{2}{\varepsilon}\dfrac{\partial H_z}{\partial y} \\[2mm]
\dfrac{\partial H_z}{\partial t} = \dfrac{2}{\mu}\dfrac{\partial E_x}{\partial y}
\end{array}
\right\} \\[8mm]
\left\{
\begin{array}{l}
\dfrac{\partial E_y}{\partial t} = \dfrac{2}{\varepsilon}\dfrac{\partial H_x}{\partial z} \\[2mm]
\dfrac{\partial H_x}{\partial t} = \dfrac{2}{\mu}\dfrac{\partial E_y}{\partial z}
\end{array}
\right\} \\[8mm]
\left\{
\begin{array}{l}
\dfrac{\partial E_z}{\partial t} = \dfrac{2}{\varepsilon}\dfrac{\partial H_y}{\partial x} \\[2mm]
\dfrac{\partial H_y}{\partial t} = \dfrac{2}{\mu}\dfrac{\partial E_z}{\partial x}
\end{array}
\right\}
\end{array}
\right\}
\quad , \quad
\left\{
\begin{array}{c}
\left\{
\begin{array}{l}
\dfrac{\partial E_x}{\partial t} = -\dfrac{2}{\varepsilon}\dfrac{\partial H_y}{\partial z} \\[2mm]
\dfrac{\partial H_y}{\partial t} = -\dfrac{2}{\mu}\dfrac{\partial E_x}{\partial z}
\end{array}
\right\} \\[8mm]
\left\{
\begin{array}{l}
\dfrac{\partial E_y}{\partial t} = -\dfrac{2}{\varepsilon}\dfrac{\partial H_z}{\partial x} \\[2mm]
\dfrac{\partial H_z}{\partial t} = -\dfrac{2}{\mu}\dfrac{\partial E_y}{\partial x}
\end{array}
\right\} \\[8mm]
\left\{
\begin{array}{l}
\dfrac{\partial E_z}{\partial t} = -\dfrac{2}{\varepsilon}\dfrac{\partial H_x}{\partial y} \\[2mm]
\dfrac{\partial H_x}{\partial t} = -\dfrac{2}{\mu}\dfrac{\partial E_z}{\partial y}
\end{array}
\right\}
\end{array}
\right\} . \tag{3.9}$$

Each of the 1-D subsystems in (3.9) can therefore very easily be solved numerically. If we choose a method which preserves the L^2-norm for each 1-D sub-problem, the sum of the squares of all the unknowns will be preserved through each sub-step, and therefore also throughout the complete computation. Unconditional numerical stability is then assured. In particular, this will be the case if we approximate each of the 1-D subsystems in (3.9) with a Crank-Nicolson type approximation. For example, to advance the first of the

six sub-problems a distance $\Delta t/4$ in time, we would use

$$\frac{E_x|_{i,j,k}^{n+\frac{1}{4}} - E_x|_{i,j,k}^n}{\Delta t/4} = \frac{2}{\epsilon}\frac{1}{2}\left\{\frac{H_z|_{i,j+1,k}^{n+\frac{1}{4}} - H_z|_{i,j-1,k}^{n+\frac{1}{4}}}{2\Delta y} + \frac{H_z|_{i,j+1,k}^n - H_z|_{i,j-1,k}^n}{2\Delta y}\right\}$$

$$\frac{H_z|_{i,j,k}^{n+\frac{1}{4}} - H_z|_{i,j,k}^n}{\Delta t/4} = \frac{2}{\mu}\frac{1}{2}\left\{\frac{E_x|_{i,j+1,k}^{n+\frac{1}{4}} - E_x|_{i,j-1,k}^{n+\frac{1}{4}}}{2\Delta y} + \frac{E_x|_{i,j+1,k}^n - E_x|_{i,j-1,k}^n}{2\Delta y}\right\}$$

If we here use the second equation to eliminate H_z on the new time level, we get a tridiagonal system to solve for E_x. Advancing (3.8) using Strang splitting together with these Crank-Nicolson approximations gives the scheme which we denote by CNS; featuring second order accuracy in time and space.

3.3.3 *Comparison between different split step sequences*

The possibility of using split step together with (3.9) for numerical time integration of Maxwell's equations was first explored in [9]. In that study, a periodic domain was used, and all the 1-D subproblems were solved analytically in (discrete) Fourier space. All errors that arose were therefore due to the time stepping, and it became possible to clearly compare the effectiveness of split step schemes of different orders. One of the observation that was made there was that different split step methods of the same order can have very different leading error coefficients. For example, seven different SS8 methods have so far been found. Fig. 3.1 shows, for a typical test problem, how the accuracy improves with increased temporal resolution. In this log-log plot, the slopes of the curves confirm the 8th order of accuracy in all cases, but the errors nevertheless differ by a full $3\frac{1}{2}$ orders of magnitude (for details about the test, see the original paper). The scheme that performs the best here - SS8d - is the one given in Table 3.1. Simply looking at the coefficients for the different schemes gives no clear indication of their difference in accuracy.

4   Enhancements to reach higher orders of accuracy in time

We have just described two possible ways to obtain second order accuracy in time combined with unconditional stability (at least for pure initial value problems): ADI and CNS. For both of these methods, at least three different procedures are available for increasing the order in time. These methods are described in each of the next three sections. This is followed by a section describing comparisons between the different combinations of basic second order methods and enhancement procedures.
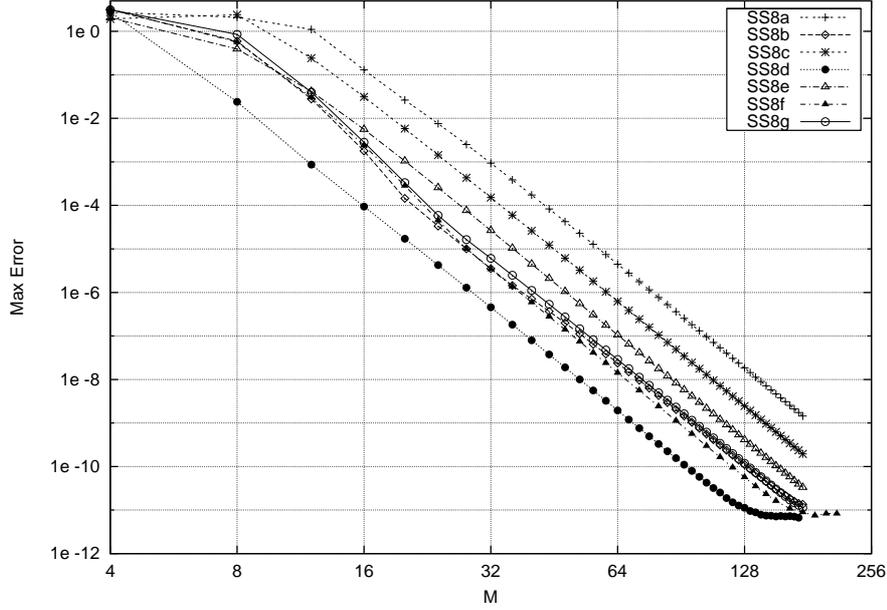
Fig. 3.1. Log-log plot comparison of error vs. number of subintervals in time for eight different SS8 methods.

4.1 Special time-step sequences

The key paper on this procedure is Yoshida [22]. We start by assuming that a globally second order accurate operator $S_2(\tau)$ advances the solution a distance τ forward in time, with a local truncation error that is expandable in the form $c_1\tau^3 + c_2\tau^5 + c_3\tau^7 + \cdots$. Then it transpires that the composite operator

$$S_4(\tau) = S_2(w_1\tau) \; S_2(w_0\tau) \; S_2(w_1\tau) \tag{4.1}$$

becomes (globally) 4th order accurate in time if the constants w_0 and w_1 are chosen as $w_0 = -\frac{2^{1/3}}{2-2^{1/3}}$ and $w_1 = \frac{1}{2-2^{1/3}}$. This idea can be continued indefinitely, with the general result stating that

$$S_{2p}(\tau) = S_2(w_k\tau) \; S_2(w_{k-1}\tau) \cdots S_2(w_1\tau) \; S_2(w_0\tau) \; S_2(w_1\tau) \cdots S_2(w_{k-1}\tau) \; S_2(w_k\tau)$$

is accurate of order $2p$ if the constants $w_k, k = 0, 1, \ldots, 2^{p-1} - 1$ satisfy certain nonlinear systems of algebraic equations. For the $p = 2$ case, the system becomes

$$\begin{cases} w_0 + 2w_1 = 1 \\ w_0^3 + 2w_1^3 = 0 \end{cases} \tag{4.2}$$

13

Table 4.1
Coefficients of some time increment sequences. See [22,9] for details.

ORDER $2p$	COEFFICIENTS $w_0, w_1, \ldots, w_k$, WHERE $k = 2^{(p-1)} - 1$		
4	-1.70241 43839 19315 26810	1.35120 71919 59657 63405	
6	1.31518 63206 83911 21888	-1.17767 99841 78871 00695	0.23557 32133 59358 13368
	0.78451 36104 77557 26382		
8	1.70845 30707 87281 58467	0.10279 98493 91796 44070	-1.96061 02329 75310 80761
	1.93813 91376 22525 98658	-0.15824 06353 68050 17520	-1.44485 22368 60605 15769
	0.25369 33365 66211 35415	0.91484 42462 29791 56675	

and in case of $p = 3$

$$
\begin{cases}
w_0 + 2(w_1 + w_2 + w_3) & = 1 \\
w_0^3 + 2(w_1^3 + w_2^3 + w_3^3) & = 0 \\
w_0^5 + 2(w_1^5 + w_2^5 + w_3^5) & = 0 \\
\big(-w_0^4 w_1 - w_0^3 w_1^2 + w_0^2 w_1^3 + w_0 w_1^4 - w_0^4 w_2 - 2w_0^3 w_1 w_2 - 2w_0 w_1^3 w_2 - 4w_1^4 w_2 \\
\quad -w_0^3 w_2^2 - 2w_1^3 w_2^2 + w_0^2 w_2^3 + 4w_0 w_1 w_2^3 + 4w_1^2 w_2^3 + w_0 w_2^4 + 2w_1 w_2^4 - w_0^4 w_3 \\
\quad -2w_0^3 w_1 w_3 - 2w_0 w_1^3 w_3 - 4w_1^4 w_3 - 2w_0^3 w_2 w_3 - 4w_1^3 w_2 w_3 - 2w_0 w_2^3 w_3 \\
\quad -4w_1 w_2^3 w_3 - 4w_2^4 w_3 - w_0^3 w_3^2 - 2w_1^3 w_3^2 - 2w_2^3 w_3^2 + w_0^2 w_3^3 + 4w_0 w_1 w_3^3 \\
\quad +4w_1^2 w_3^3 + 4w_0 w_2 w_3^3 + 8w_1 w_2 w_3^3 + 4w_2^2 w_3^3 + w_0 w_3^4 + 2w_1 w_3^4 + 2w_2 w_3^4\big) & = 0
\end{cases}
\tag{4.3}
$$

Convenient recursive expressions to create the algebraic system for the general order of accuracy $2p$ are given in [22]. These are well suited both for numerical computations of solutions and for more analytic exploration of the systems by means of computational symbolic algebra. Since the number of steps in these time-step sequences increase exponentially with the order, fairly low orders are probably of most interest. Table 4.1, will therefore suffice for most needs. We give here one example of solutions for each order (choosing for the 8th order the scheme that corresponds to the split step scheme that was most effective in the comparison shown in Fig. 3.1). Coefficients for all presently known schemes up to and including 8th order can be found in [9]. If we apply these time incremental sequences to any Strang split SS2 method, we get the methods we earlier described as SS4, SS6, etc. But the sequences can just as well be applied to other second order time stepping methods, such as the ADI and CNS method. In this study, we use ADI and CNS as the two 'basic' second order schemes (sometimes denoted ADI2 and CNS2 to remind about their accuracy). The time sequence enhancements of these methods (based on the coefficients in Table 4.1) will be denoted ADI-TSq and CNS-TSq respectively, where q is the resulting order in time.

We conclude this section by briefly indicating how the systems (4.2) etc. can be obtained. If X and Y are operators (or matrices) that commute, then $e^X \cdot e^Y = e^Z$ with $Z = X + Y$. If X and Y do not commute, the expression for Z becomes far more complicated. By the Baker-Campbell-Hausdorff (BCH)

formula [20]

$$Z = (X + Y) + [X, Y]$$

$$+ \frac{1}{12} \left([X, X, Y] + [Y, Y, X] \right)$$

$$+ \frac{1}{24} [X, Y, Y, X] \tag{4.4}$$

$$+ \left\{ \begin{array}{l} \text{commutators of successi-} \\ \text{vely increasing orders} \end{array} \right\},$$

where $[X, Y] = X\,Y - Y\,X$, $[X, Y, V] = [X, [Y, V]]$, etc. Repeated application of (4.4) gives $e^X \cdot e^Y \cdot e^X = e^W$ where

$$W = (2X + Y) + \tfrac{1}{6} \left([Y, Y, X] - [X, X, Y] \right)$$

$$+ \left\{ \begin{array}{l} \text{commutators of successi-} \\ \text{vely increasing orders} \end{array} \right\}. \tag{4.5}$$

With our assumption that the operator $S_2(\tau)$ advances the equation $u' = Au$ the distance τ in time, with a local error of $c_1 \tau^3 + c_2 \tau^5 + \cdots$, it can be written $S_2(\tau) = e^{\tau A + \tau^3 B + O(\tau^5)}$. The RHS of (4.1) becomes then

$$\overbrace{e^{(w_1 \tau)A + (w_1 \tau)^3 B + O(\tau^5)}}^{X} \cdot \overbrace{e^{(w_0 \tau)A + (w_0 \tau)^3 B + O(\tau^5)}}^{Y} \cdot \overbrace{e^{(w_1 \tau)A + (w_1 \tau)^3 B + O(\tau^5)}}^{X} .$$

By (4.5) this becomes

$$\overbrace{e^{(2w_1 + w_0)\tau A + (2w_1^3 + w_0^3)\tau^3 B + O(\tau^5)}}^{2X + Y} + \overbrace{O(\tau^5)}^{\text{higher terms}} .$$

This represents a 4th order method if it is of the form $e^{\tau A + O(\tau^5)}$, i.e. if (4.2) holds. To reach higher orders, we need to extend the BCH formula to products of still more exponentials. When the commutators also come into play for some of the relations that need to be satisfied, the complexity of the resulting algebraic equations rapidly increase, as is seen in (4.3). However, as we noted just above, the original reference [22] shows that the higher order systems can be obtained recursively very conveniently.

The idea, going back to Lewis Fry Richardson in 1927 [16], has been used since then in many applications, e.g. in extrapolation methods for ODEs, and as Romberg's method for quadrature. If we have a numerical procedure for which the error of a computed variable u depends on a step size h in the following way

$$u_h = Exact + c_1 h^2 + c_2 h^4 + \cdots$$

then repeating his calculation using a step size $h/2$ will give

$$u_{h/2} = Exact + c_1 \tfrac{1}{4} h^2 + c_2 \tfrac{1}{16} h^4 + \cdots$$

These two results can then be linearly combined to eliminate $c_1 h^2$, giving the more accurate result

$$v_{h/2} = \frac{4\, u_{h/2} - u_h}{3} = Exact - c_2 \tfrac{1}{4} h^4 + \cdots$$

This idea can be continued repeatedly, and the results are conveniently laid out in triangular form

DIRECTLY COMPUTED	EXTRAPOLATED		
ORDER 2	ORDER 4	ORDER 6	ORDER 8
u_h			
$u_{h/2}$	$v_{h/2} = \frac{4u_{h/2} - u_h}{3}$		
$u_{h/4}$	$v_{h/4} = \frac{4u_{h/4} - u_{h/2}}{3}$	$w_{h/4} = \frac{16v_{h/4} - v_{h/2}}{15}$	
$u_{h/8}$	$v_{h/8} = \frac{4u_{h/8} - u_{h/4}}{3}$	$w_{h/8} = \frac{16v_{h/8} - v_{h/4}}{15}$	$x_{h/8} = \frac{64w_{h/8} - w_{h/4}}{63}$
$\vdots$	$\vdots$	$\vdots$	$\vdots$

In the context of quadrature, it is common practice to halve the step between each calculation (as we assumes above in order to be able to re-use as many old function values as possible). The drawback with that strategy is that, like for the approach with special time step sequences, the work grows exponentially with the order. In the context of ODEs - which essentially is our situation when time stepping the Maxwell's equations - it is much preferable to make smaller changes in the time step between the different computations. The extrapolation procedure will still increase the order by two for each new original computation, but without the need of each computation to be twice as expensive as the previous one. In the following, we will use this extrapolation approach to enhance the ADI method, and denote the results ADI-EXq where again, q denotes the resulting order.

4.3   Deferred correction

This concept of deferred correction was introduced by Pereyra [15], first in the context of solving 2-point boundary value problems for ODEs, and was used subsequently for solutions of PDEs. Gustafsson and Kress [7] use the method for increasing the order of accuracy in the time stepping of ODEs, and they illustrate the effectiveness of this for a methods-of-lines solution of a 1-D heat equation. We will describe it here in the context of our ADI scheme. The procedure to increase the temporal order of accuracy from 2 to 4 consists of the following steps:

- Step the ADI2 scheme over some time interval $[0, T]$.
- Using the numerical values from this solution, evaluate an approximation of the local truncation error $\underline{E}^{n+1/2}$ at each time level.
- Re-run the ADI2 scheme over the time $[0, T]$, but include $\underline{E}^{n+1/2}$ as a RHS (a forcing function) to the equation.

The last two steps can be repeated in order to reach still higher orders of accuracy (6, 8, ...). Two orders of accuracy will be gained each time the basic second order scheme is re-run. We will denote the enhancement of the ADI method using deferred correction as ADI-DCq where q is the resulting order.

To apply this idea to the ADI scheme, we start by noting that the local error in (3.5) becomes

$$
\begin{aligned}
\underline{E}^{n+\frac{1}{2}} &= \left(1 - \frac{\Delta t}{2}A\right)\left(1 - \frac{\Delta t}{2}B\right)\underline{u}^{n+1} - \left(1 + \frac{\Delta t}{2}A\right)\left(1 + \frac{\Delta t}{2}B\right)\underline{u}^{n} \\
&= \left(1 + \frac{(\Delta t)^2}{4}AB\right)\left(\underline{u}^{n+1} - \underline{u}^{n}\right) - \frac{\Delta t}{2}\left(\underline{u}^{n+1} + \underline{u}^{n}\right).
\end{aligned}
$$

From the expansions

$$
\underline{u}^{n+1} - \underline{u}^{n} = \Delta t\, \underline{u}_t^{n+\frac{1}{2}} + \frac{(\Delta t)^3}{24}\underline{u}_{ttt}^{n+\frac{1}{2}} + \frac{(\Delta t)^5}{1920}\underline{u}_{ttttt}^{n+\frac{1}{2}} + \cdots,
$$

$$
\underline{u}^{n+1} + \underline{u}^{n} = 2\underline{u}^{n+\frac{1}{2}} + \frac{(\Delta t)^2}{4}\underline{u}_{tt}^{n+\frac{1}{2}} + \frac{(\Delta t)^4}{192}\underline{u}_{tttt}^{n+\frac{1}{2}} + \cdots
$$

17

we obtain the following error expansion;

$$
\underline{E}^{n+\frac{1}{2}} = \left(\underline{u}_t^{n+\frac{1}{2}} - (A+B)\underline{u}^{n+\frac{1}{2}} \right) \Delta t
$$

<div style="text-align:right">Vanishes
because
of the PDE</div>

$$
+ \left(\frac{AB}{4}\underline{u}_t^{n+\frac{1}{2}} - \frac{A+B}{8}\underline{u}_{tt}^{n+\frac{1}{2}} + \frac{1}{24}\underline{u}_{ttt}^{n+\frac{1}{2}} \right) (\Delta t)^3
$$

<div style="text-align:right">Use to get
DC of
order 4</div>

$$
+ \left(\frac{AB}{96}\underline{u}_{ttt}^{n+\frac{1}{2}} - \frac{A+B}{384}\underline{u}_{tttt}^{n+\frac{1}{2}} + \frac{1}{1920}\underline{u}_{ttttt}^{n+\frac{1}{2}} \right) (\Delta t)^5
$$

<div style="text-align:right">Use to get
DC of
order 6</div>

$$
+ \cdots .
$$

<div style="text-align:right">...</div>

(4.6)

To get from ADI2 to ADI-DC4, we would approximate $\underline{E}^{n+1/2}$ by

$$
\underline{E}^{n+\frac{1}{2}} \approx \frac{(\Delta t)^2}{4} AB(\underline{u}^{n+1} - \underline{u}^n) - \frac{\Delta t}{16}(\underline{u}^{n+2} - \underline{u}^{n+1} - \underline{u}^n + \underline{u}^{n-1}) +
$$
$$
\frac{1}{4}(A+B)(\underline{u}^{n+2} - 3\underline{u}^{n+1} + 3\underline{u}^n - \underline{u}^{n-1}).
$$

For ADI-DC6, we approximate $\underline{E}^{n+1/2}$ with a 4th order finite difference for time derivatives of the second term using the numerical values from ADI2, and with 2nd order finite difference for time derivatives of the third term, using the numerical values from ADI-DC4 in the RHS of (4.6).

Similarly to how we obtained (3.6) from (3.5), it follows that

$$
\left(1 - \frac{\Delta t}{2}A\right)\left(1 - \frac{\Delta t}{2}B\right)\underline{u}^{n+1} = \left(1 + \frac{\Delta t}{2}A\right)\left(1 + \frac{\Delta t}{2}B\right)\underline{u}^n + \underline{E}^{n+\frac{1}{2}} \quad (4.7)
$$

is equivalent to

$$
\begin{cases} \left(1 - \dfrac{\Delta t}{2}A\right)\underline{u}^{n+\frac{1}{2}} = \left(1 + \dfrac{\Delta t}{2}B\right)\underline{u}^n \quad + \dfrac{1}{2}\underline{E}^{n+\frac{1}{2}} \\[2ex] \left(1 - \dfrac{\Delta t}{2}B\right)\underline{u}^{n+1} = \left(1 + \dfrac{\Delta t}{2}A\right)\underline{u}^{n+\frac{1}{2}} + \dfrac{1}{2}\underline{E}^{n+\frac{1}{2}} \end{cases} . \quad (4.8)
$$

Multiplying the second equation in (4.8) by $\left(1 - \dfrac{\Delta t}{2}A\right)$ and then using the first equation in (4.8) leads to (4.7).

The corrections in this deferred correction procedure can therefore be very conveniently implemented by applying half the amount of the approximate local error to each of the two ADI stages.

5   Further enhancements

For ADI-EX and ADI-DC procedures, we can increase the accuracy significantly at very little extra extra cost as follows:

- Divide the time interval $I = [0, T]$ into a finite number of subintervals such that $I = \cup_{k=1}^{k=q}[t_{k-1}, t_k]$, $t_0 = 0$, $t_q = T$, where t_k, $k > 1$ is a positive integer multiple of the given time stepping size Δt.
- Approximate numerical solution at each time level in $[t_0, t_1]$ using ADI-EX or ADI-DC.
- For $k = 1, \ldots, q-1$, restart the corresponding method using the numerical values obtained (high order accurate) at t_k as the initial condition for the next subinterval $[t_k, t_{k+1}]$.

We denote these enhanced method as ADI-REX or ADI-RDC, where "R" stands for "re-started". The methods will be discussed further in Section 6.2.

6   Numerical experiments and comparisons

The time stepping methods we have just introduced and which we will now proceed to compare are

- ADI2 and CNS2: The 'basic' second order methods described in Section 3.
- ADI-TS and CNS-TS: Enhancements of ADI2 and CNS2, using the time sequence enhancements described in Section 4.1.
- ADI-EX: Extrapolations of ADI2, as described in Section 4.2.
- ADI-DC: Deferred corrections of ADI2, as described in Section 4.3.
- ADI-REX and ADI-RDC: Methods involving restarting ADI-EX and ADI-DC on each temporal subinterval, as described in Section 5.

The number at the end of each method denotes the order of accuracy in time of each method.
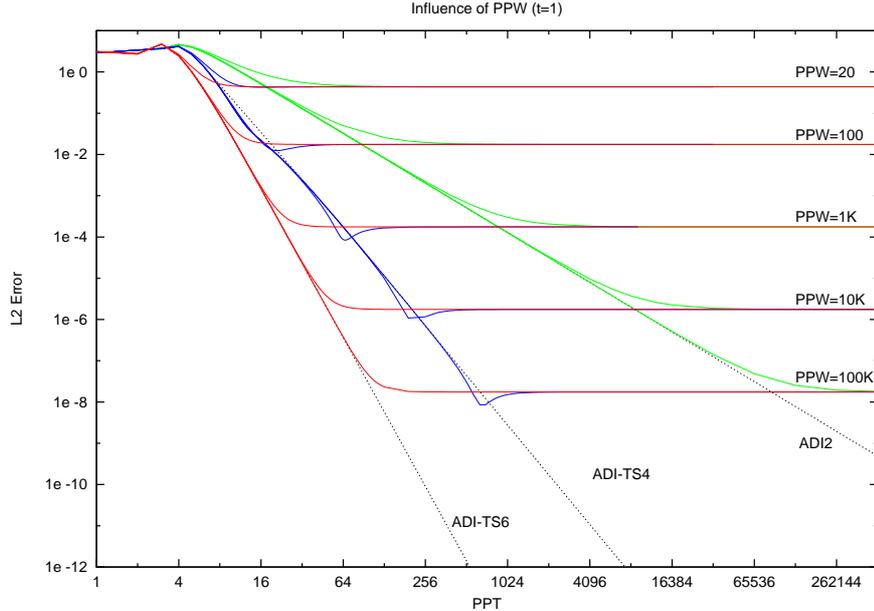
Fig. 6.1. Log-log plot: influence of PPW (spatial discretization), and comparison of L_2-errors (solid lines) vs. PPT for ADI2, ADI-TS4, and ADI-TS6. Dotted lines (corresponding to PPW $= \infty$) are obtained using linear extrapolations. The letter K stands for 1000.

For the numerical experiments, we choose the following exact periodic solution of the equation (2.1) over the unit cube with $\varepsilon = \mu = 1$:

$$
\begin{aligned}
E_x &= \cos(2\pi(x + y + z) - 2\sqrt{3}\pi t), & H_x &= \sqrt{3}E_x, \\
E_y &= -2E_x, & H_y &= 0, \\
E_z &= E_x, & H_z &= -\sqrt{3}E_x.
\end{aligned}
\tag{6.1}
$$

This corresponds to waves propagating along the main diagonal of the computational lattice. As shown in [1] (Fig. 2, left part), the anisotropy of the ADI scheme is fairly weak, with only about a factor of two difference in errors between different propagation directions. Hence, we limit the comparisons here to a single direction.

We approximate the solution of the 3-D Maxwell's equations (2.1) in Fourier space over a uniform spatial grid. All spatial discretizations of the methods we test are 2nd order accurate. The semi-discrete problem for (2.1) then reduces to $\underline{u}_t^h = \mathcal{A}\underline{u}^h$ for a 6x6 matrix $\mathcal{A}$ The fully discrete version depends on the time stepping approach and on 2 parameters, which we choose as points per time interval $(0, T]$ (PPT) and points per wave length (PPW). We then compare using the L_2-norm the analytic solution (6.1) to the computed discrete approximation. Our Fourier space approach for the numerics allows us to see the influence of the PPW quantity (i.e. the spatial discretization) also for very high PPW without incurring any increased computational expense.

20
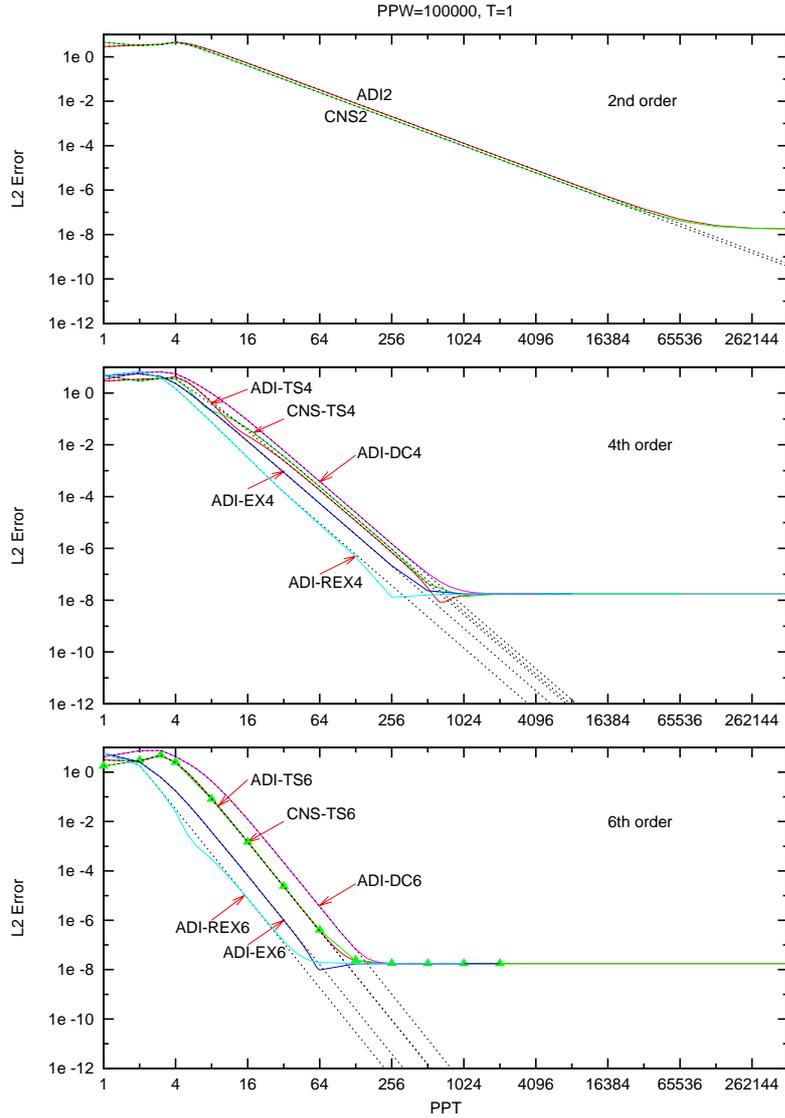
Fig. 6.2. Log-log plot comparison of performance without cost adjustment. For clarity, methods are grouped by order. Solid lines are error curves for PPW=100,000; dotted lines (corresponding to PPW = ∞) are obtained using linear extrapolations. The curve with filled triangle is that of CNS-TS6, which is graphically indistinguishable with that of ADI-TS6. The curves for ADI-REX are obtained using PPT subintervals (i.e., the extreme case of re-starting after each time step).

6.1 Short-time error and cost comparisons

Fig. 6.1 shows that influence of PPW for ADI2, ADI-TS4, and ADI-TS6. Using data for various PPW, we extrapolate linearly to obtain dotted curves corresponding to infinite number of PPW for those methods. Similarly we obtain error curves corresponding to infinite number of PPW for the other methods. The value of PPW controls the spatial error, and therefore limits
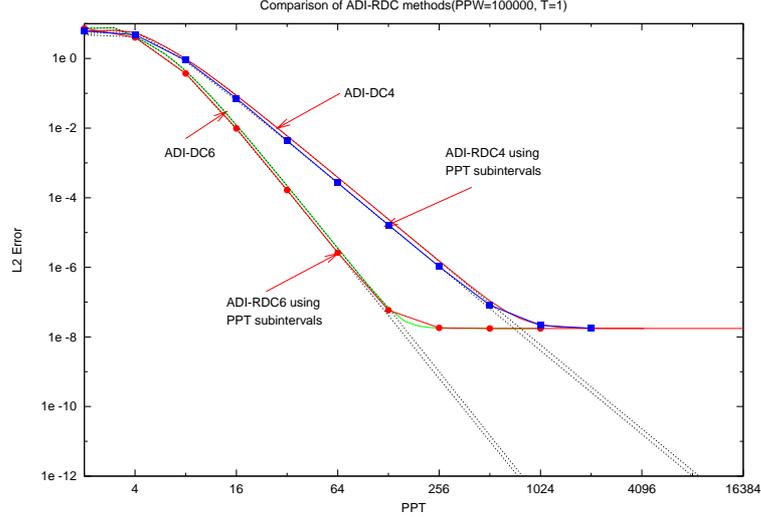
Fig. 6.3. Log-log plot comparison of performance without cost adjustment of ADI-RDC methods. Solid lines are error curves for PPW=100,000; dotted lines (corresponding to PPW = ∞) are obtained using linear extrapolations. The curves with filled circles and rectangles are are those of ADI-RDC6 and ADI-RDC4 obtained using PPT subintervals, respectively. Curves for ADI-RDC using different PPTs fall between two curves with the same slopes. In this hsort run, re-starts are seem to offer little or no benefits.

the overall accuracy that can be reached (independently of how the time stepping is carried out). Since we are interested in very high PPW, we will in the following figures usually choose PPW $= 10^5$ and with dotted lines indicate the PPW $= \infty$ error curves. In a few cases (Figs 6.4 and 6.5) we also mark the floors imposed by lower values of PPW. Fig. 6.2 compares the performances of the methods as smaller time steps are used (higher PPT - points during total time). Fig. 6.3 displays accuracy for ADI-RDC. The slopes of the curves confirm that the order of accuracy in time is as expected. We measure the computational cost in units of floating point operations required for one full ADI2 time step (assuming tridiagonal linear systems are solved with the standard Thomas algorithm, i.e. unpivoted tridiagonal Gaussian elimination). Fig. 6.4 shows how the accuracy at the final time $T = 1$ improves as smaller time steps are used (in terms of amount of work equivalent for ADI2). The dotted horizontal lines denote accuracy obtainable using given number of PPW.

For these comparisons, we note:

- Our CNS2 method is comparable to ADI2.
- For each time stepping method, the efficiency improves with the order of accuracy. The improvement is dramatic in moving from order 2 to 4, but levels off somewhat in going further to order 6.
- As higher level of accuracy is needed, higher order methods are more effective.
- Comparing methods of the same accuracy of order, ADI-REX method is
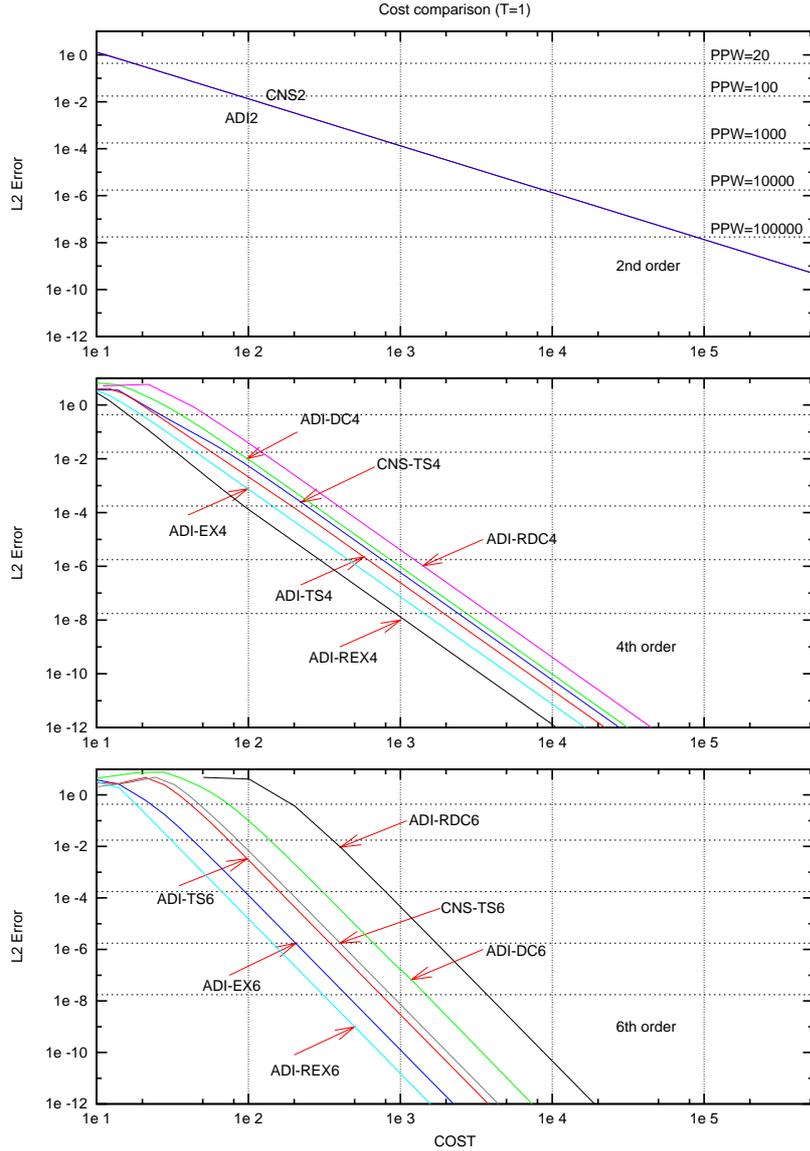
Fig. 6.4. Log-log plot comparison of performance with cost adjustment. For clarity, methods are grouped by order. Each line is corresponding to the case of PPW $= \infty$. The curves for ADI-REX and ADI-RDC are obtained using PPT subintervals. The horizontal axis represents the work amount equivalent to the cost of ADI2. The dotted horizontal lines are the accuracy obtainable using given number of PPW.

most cost effective among methods tested. In particular, ADI-REX6 is superior to the other methods tested in almost all ranges of accuracy levels.

- Of the three enhancement methods, extrapolation appears to be the most effective, followed by the time sequence procedure.
- Figs 6.3 and 6.4 show that during this short run, there is no benefit by re-starting.

23
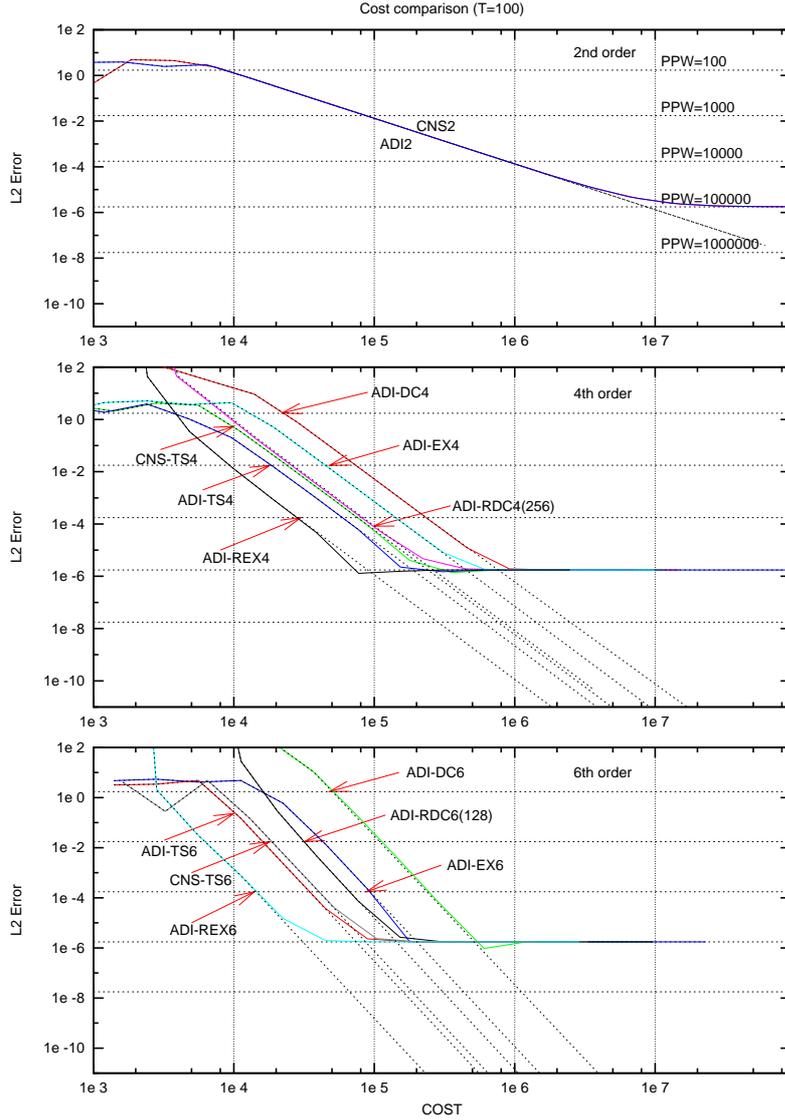
Fig. 6.5. Log-log plot comparison of performance with cost adjustment. For clarity, methods are grouped by order. Solid lines are error curves for PPW=100,000; dotted lines (corresponding to PPW = ∞) are obtained using linear extrapolations. The curves for ADI-REX are obtained using PPT subintervals and the number in the parenthesis of ADI-RDC methods is the number of subintervals used. The horizontal axis denotes cost equivalent work amount of ADI2. The dotted horizontal lines are the accuracy obtainable using given number of PPW.

6.2 Long time behaviors

The final time is now changed from $T = 1$ to $T = 100$. Fig. 6.5 shows the performance of each time stepping method with work adjustment included. Tables 6.1 and 6.2 show the accuracy of ADI-REX method and Tables 6.3 and 6.4 show the accuracy of ADI-RDC method. We notice that re-starting

TABLE 6.1

Performance of ADI-REX4: L_2-error of the approximated solution with $PPW = 100{,}000$ at the final time $T = 100$ is about 0.175×10^{-5}.

	ADI-REX4 with PPW=100,000											
	Number of subintervals											
PPT	1	2	4	8	16	32	64	128	256	512	1024	PPT
2048	.653 e 1	.675 e 1	.178 e 2	.137 e 2	.545 e 1	.211 e 1	.917 e 0	.439 e 0	.235 e 0	.179 e 0	.154 e 0	.108 e 0
4096	.247 e 1	.166 e 1	.861 e 0	.417 e 0	.203 e 0	.998 e-1	.500 e-1	.256 e-1	.142 e-1	.108 e-1	.933 e-2	.523 e-2
8192	.193 e 0	.986 e-1	.493 e-1	.246 e-1	.123 e-1	.614 e-2	.310 e-2	.160 e-2	.891 e-3	.676 e-3	.581 e-3	.297 e-3
16384	.122 e-1	.613 e-2	.306 e-2	.153 e-2	.767 e-3	.384 e-3	.194 e-3	.100 e-3	.561 e-4	.431 e-4	.365 e-4	.165 e-4
32768	.766 e-3	.383 e-3	.192 e-3	.958 e-4	.480 e-4	.241 e-4	.124 e-4	.677 e-5	.424 e-5	.295 e-5	.172 e-5	.636 e-6
65536	.479 e-4	.240 e-4	.121 e-4	.625 e-5	.350 e-5	.235 e-5	.196 e-5	.186 e-5	.182 e-5	.177 e-5		.168 e-5
131072	.347 e-5	.231 e-5	.191 e-5	.180 e-5	.177 e-5	.176 e-5	.176 e-5	.176 e-5	.176 e-5	.185 e-5	.175 e-5	.175 e-5
262144	.176 e-5	.176 e-5	.175 e-5	.175 e-5	.175 e-5	.175 e-5	.175 e-5	.175 e-5	.175 e-5	.175 e-5	.175 e-5	.175 e-5

TABLE 6.2

Performance of ADI-REX6: L_2-error of the approximated solution with $PPW = 100{,}000$ at the final time $T = 100$ is about 0.175×10^{-5}.

	ADI-REX6 with PPW=100,000											
	Number of subintervals											
PPT	1	2	4	8	16	32	64	128	256	512	1024	PPT
512	.110 e 1	.100 e 1	.278 e 2	.689 e 2	.192 e 5	.209 e 5	.903 e 2	.415 e 1	.116 e 1	.194 e 0	....	.194 e 0
1024	.697 e 1	.733 e 1	.269 e 2	.242 e 2	.433 e 1	.827 e 0	.202 e 0	.501 e-1	.147 e-1	.267 e-2	.881 e-2	.881 e-2
2048	.278 e 1	.208 e 1	.770 e 0	.202 e 0	.511 e-1	.129 e-1	.324 e-2	.826 e-3	.231 e-3	.338 e-4	.146 e-3	.181 e-3
4096	.177 e 0	.502 e 0	.129 e-1	.325 e-2	.812 e-3	.203 e-3	.495 e-4	.116 e-4	.319 e-5	.130 e-5	.397 e-5	.472 e-5
8192	.323 e-2	.812 e-3	.202 e-3	.493 e-4	.110 e-4	.149 e-5	.100 e-5	.173 e-5	.175 e-5	.179 e-5	.180 e-5	.180 e-5
16384	.493 e-4	.110 e-4	.143 e-5	.957 e-6	.155 e-5	.170 e-5	.174 e-5	.175 e-5	.175 e-5	.175 e-5	.175 e-5	.175 e-5
32768	.956 e-6	.155 e-5	.170 e-5	.174 e-5	.175 e-5	.175 e-5	.175 e-5	.175 e-5	.175 e-5	.175 e-5	.175 e-5	.175 e-5

TABLE 6.3

Performance of ADI-RDC4: L_2-error of the approximated solution with $PPW = 100,000$ at the final time $T = 100$ is about 0.175×10^{-5}.

| | ADI-RDC4 with PPW=100,000 | | | | | | | | | | | |
| | Number of subintervals | | | | | | | | | | | |
PPT	1	2	4	8	16	32	64	128	256	512	1024	2048
2048	.280 e 2	.863 e 2	.213 e 3	.221 e 3	.724 e 2	.177 e 2	.661 e 1	.402 e 1	.320 e 1	.314 e 1	.286 e 1	
4096	.918 e 1	.784 e 1	.442 e 1	.200 e 1	.912 e 0	.461 e 0	.280 e 0	.218 e 0	.194 e 0	.200 e 0	.179 e 0	.162 e 0
8192	.767 e 0	.403 e 0	.201 e 0	.100 e-1	.507 e-1	.273 e-1	.171 e-1	.136 e-1	.122 e-1	.126 e-1	.113 e-1	.102 e-1
16384	.489 e-1	.245 e-1	.123 e-1	.617 e-2	.315 e-2	.171 e-2	.107 e-2	.852 e-3	.767 e-3	.790 e-3	.644 e-3	.622 e-3
32768	.306 e-2	.153 e-2	.767 e-3	.386 e-3	.198 e-3	.107 e-3	.684 e-4	.548 e-4	.496 e-4	.510 e-4	.460 e-4	.149 e-4
65536	.192 e-3	.959 e-4	.481 e-4	.244 e-4	.129 e-4	.760 e-5	.556 e-5	.495 e-5	.470 e-5	.482 e-5	.450 e-5	.425 e-5
131072	.121 e-4	.629 e-5	.356 e-5	.245 e-5	.208 e-5	.197 e-5	.195 e-5	.194 e-5	.193 e-5	.194 e-5	.192 e-5	.191 e-5
262144	.192 e-5	.180 e-5	.178 e-5	.177 e-5	.177 e-5	.177 e-5	.177 e-5	.177 e-5	.177 e-5	.177 e-5	.176 e-5	.176 e-5
524288	.176 e-5	.175 e-5	.175 e-5	.175 e-5	.175 e-5	.175 e-5	.175 e-5	.175 e-5	.175 e-5	.175 e-5	.175 e-5	.175 e-5

TABLE 6.4

Performance of ADI-RDC6: L_2-error of the approximated solution with $PPW = 100,000$ at the final time $T = 100$ is about 0.175×10^{-5}.

| | ADI-RDC6 with PPW=100,000 | | | | | | | | | | | |
| | Number of subintervals | | | | | | | | | | | |
PPT	1	2	4	8	16	32	64	128	256	512	1024	2048
2048	.175 e 3	.768 e 3	.113 e 4	.922 e 2	.536 e 1	.109 e 1	.423 e 0	.280 e 0	.250 e 0	.243 e 0	.235 e 0	
4096	.107 e 2	.403 e 1	.872 e 0	.209 e 0	.539 e-1	.158 e-1	.671 e-2	.459 e-2	.417 e-2	.408 e-2	.396 e-2	.380 e-2
8192	.205 e 0	.518 e-1	.130 e-1	.329 e-2	.856 e-3	.252 e-3	.107 e-3	.744 e-4	.680 e-4	.668 e-4	.648 e-4	.624 e-4
16384	.326 e-2	.815 e-3	.203 e-3	.500 e-4	.120 e-4	.334 e-5	.258 e-5	.269 e-5	.274 e-5	.276 e-5	.274 e-5	.270 e-5
32768	.493 e-4	.110 e-4	.149 e-5	.996 e-6	.157 e-5	.172 e-5	.176 e-5	.177 e-5	.177 e-5	.177 e-5	.177 e-5	.177 e-5
65536	.957 e-6	.155 e-5	.170 e-5	.174 e-5	.175 e-5	.175 e-5	.175 e-5	.175 e-5	.175 e-5	.175 e-5	.175 e-5	.175 e-5
131072	.174 e-5	.175 e-5	.175 e-5	.175 e-5	.175 e-5	.175 e-5	.175 e-5	.175 e-5	.175 e-5	.175 e-5	.175 e-5	.175 e-5

now in some cases is very beneficial. As the number of subintervals is doubled the accuracy in some cases increases by a factor 2 for ADI-REX4 and ADI-RDC4 and by a factor 4 for ADI-REX6 and ADI-RDC6 (up to certain number of subintervals). We can further note:

- For each time stepping method, the efficiency improves with the order of accuracy, as was the case for $T = 1$.
- Comparing methods of the same accuracy of order, ADI-REX method is most cost effective among methods tested. ADI-RDC method shows better performance than for $T = 1$. However, also for long time integration, ADI-REX6 is superior to the other methods tested in almost all ranges of accuracy levels.

7 An example with material interfaces

In order to evaluate the performance of Richardson extrapolations in time stepping for problems with material interfaces, we numerically solve the following one dimensional Maxwell's equations (7.1) for transverse magnetic (TM) waves in presence of material objects, and compare accuracy of ADI2, ADI-EX4 and ADI-EX6.

$$\begin{cases} \dfrac{\partial E_z}{\partial t} = \dfrac{1}{\varepsilon}\dfrac{\partial H_y}{\partial x} \\[2mm] \dfrac{\partial H_y}{\partial t} = \dfrac{1}{\mu}\dfrac{\partial E_z}{\partial y} \end{cases}. \tag{7.1}$$

We solve an initial boundary value problem associated with (7.1) on the unit interval $[0, 1]$ with perfect electric conductors at both ends and a dielectric medium given by

$$\varepsilon(x) = \begin{cases} 4, & 0.1 \le x \le 0.2, \\[2mm] 1, & 0 \le x \le 1, \end{cases} \tag{7.2}$$

$$\mu(x) = 1.$$

In this test, the following Gaussian pulse is used as the initial condition.

$$\begin{cases} E_z(x, 0) = \exp\left(-\alpha(x - x_0)^2\right) \\[4mm] H_y(x, 0) = \sqrt{\dfrac{\mu_0}{\varepsilon_0}} E_z(x, 0) \end{cases},$$

where $\alpha = 800, x_0 = 0.7, \epsilon_0 = 1, \mu_0 = 1$.

As mentioned in Section 1 and in view of points made in the previous section,

27
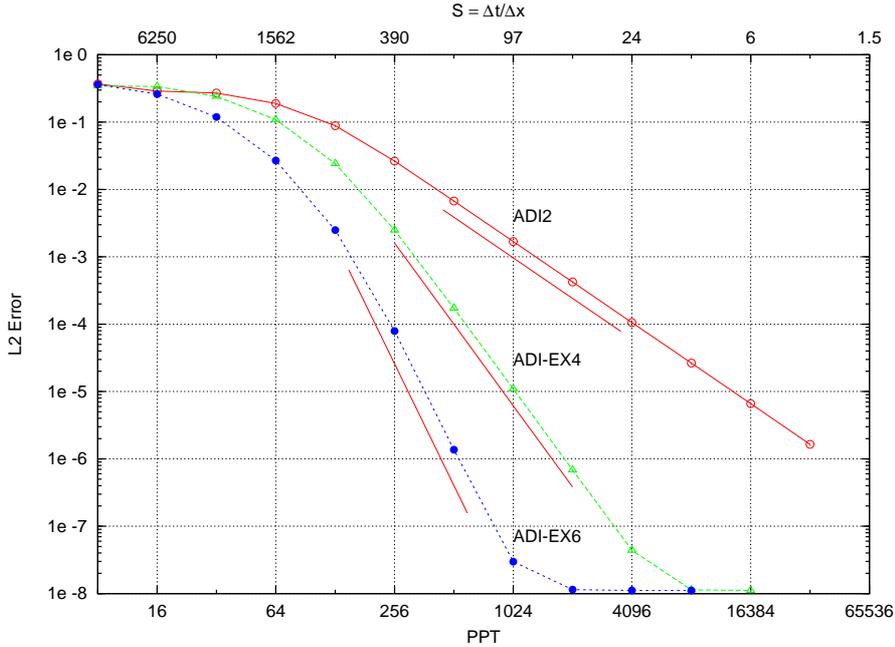
Fig. 7.1. Log-log plot: L_2-errors at $T = 1$ of ADI2, ADI-EX4, and ADI-EX6 as functions of PPT for the one dimensional Maxwell's equations (7.1) for transverse magnetic waves in the unit interval $[0, 1]$ with perfect electric conductors at both end and a discontinuous medium given by (7.2). The upper horizontal represents the ratio $S = \Delta t / \Delta x$. The corresponding CFL limit of Yee scheme to this problem is $S = 1$. In order to compare accuracy, we use the numerical solution obtained with $\Delta x = 1/100,000$ and $S = 0.25$ as the reference solution. Each solid line segment represents the slope of the convergence rate 2, 4, and 6, respectively, from above.

we numerically solve, using ADI2, ADI-EX4, and ADI-EX6, the problem with $\Delta x = 1/100,000$ (spatially over resolved) and various values of $S = \Delta t / \Delta x$ to see how the temporal accuracy improves as smaller time steps are used. We choose the numerical solution obtained by using $\Delta x = 1/100,000, \Delta t = \Delta x/4$ as the reference solution to compare accuracy of methods tested.

Fig. 7.1 displays accuracy for ADI2, ADI-EX4 and ADI-EX6 at the final time $T = 1$. The slopes of the curves confirm that the order of accuracy in time is as expected. Noting that the corresponding CFL limit of Yee scheme to this test problem is $S = 1$, the absence of divergence when S is several thousand times larger strongly supports the notion that unconditional stability is retained. Therefore extrapolations for time stepping may improve the order of accuracy for problems with material interfaces.

8   Conclusions

In this study we have noted that there now exist two different (but related) unconditionally stable time stepping procedures for the 3-D Maxwell's equa-

tions, which both require only the solution of tridiagonal linear systems: ADI2 and CNS2. We then introduced three different procedures for enhancing the temporal accuracy for these two schemes to higher orders - Richardson extrapolation, special time step sequences, and deferred correction in time. Of these three, Richardson extrapolation appeared in all cases to be the most cost effective choice. It is again unconditionally stable (at least as long as the number of re-starts is kept fixed) since it only amounts to a finite linear combination of known unconditionally stable ADI2- (or CNS2-) results.

With these results established, several additional directions of study will be pursued:

- Further stability analysis of the enhanced time stepping procedures. For example, although the unconditional stability is clear for Richardson extrapolation and deferred correction with a finite number of re-starts, the influence of increasingly many re-starts is unclear. The special time sequence (TSq) methods appears to be unconditionally stable for $q = 4$, but not higher.
- Application of proposed methods to cases with more realistic boundary conditions and/or media with varying electromagnetic properties. In such cases, it was suggested in [6] that the product AB appearing in (3.4) - and not present in non-split schemes - could possibly become a notable error source that does not show up in constant coefficient dispersion analysis. The enhanced time stepping methods introduced here ought to eliminate - to leading order - this error term. This needs to be numerically verified.
- The Maxwell's equations (2.1) imply conservation of $\nabla \cdot \mathbf{E}$ and $\nabla \cdot \mathbf{H}$, where $\mathbf{E}$ and $\mathbf{H}$ are the electric and magnetic field, respectively. The numerical conservation of the corresponding quantities hold exactly for the Yee schemes, but usually not for other schemes. The significance of non-conservation remains unclear.

References

[1] M. DARMS, R. SCHUHMANN, H. SPACHMANN, AND T. WEILAND, *Asymmetry effects in the ADI-FDTD algorithm*, IEEE Microwave Guided Wave Lett., 12 (2002), pp. 491–493.

[2] J. DOUGLAS, JR., *On the numerical integration of $\frac{\partial^2 u}{\partial x^2} + \frac{\partial^2 u}{\partial y^2} = \frac{\partial u}{\partial t}$ by implicit methods*, J. Soc. Indust. Appl. Math., 3 (1955), pp. 42–65.

[3] B. FORNBERG, *A short proof of the unconditional stability of the ADI-FDTD scheme*, University of Colorado, Department of Applied Mathematics Technical Report # 472, (2001).

[4] ——, *Some numerical techniques for Mawell's equations in different type of geometries*, in Topics in Computational Wave Propagation 2002, Springer, (2003), pp. 265–299

[5] B. FORNBERG AND T. DRISCOLL, *A fast spectral algorithm for nonlinear wave equations with linear dispersion*, J. Comp. Phys., 155 (1999), pp. 456–467.

[6] S. GARCÍA, T.-W. LEE, AND S. HAGNESS, *On the Accuracy of the ADI-FDTD method*, IEEE Antennas and Wireless Propagat. Lett., (2003), pp. 31–34.

[7] B. GUSTAFSSON AND W. KRESS, *Deferred correction methods for initial value problems*, BIT, 41 (2001), pp. 986–995.

[8] K. KUNZ AND J. LUEBBERS, *The Finite-Difference Time-Domain Method for Electromagnetics*, CRC Press, Inc., 1993.

[9] J. LEE AND B. FORNBERG, *A Split step Approach for the 3-D Maxwell's equations*, J. Comput. Appl. Math., 158 (2003), pp. 485–505.

[10] G. LIU AND S. GEDNEY, *Perfectly matched layer media for an unconditionally stable three-dimensional ADI-FDTD method*, IEEE Microwave Guided Wave Lett., 10 (2000), pp. 261–263.

[11] J. MAXWELL, *A Treatise on Electricity and Magnetism*, Clarendon Press, Oxford, 1873.

[12] T. NAMIKI, *3-D ADI-FDTD method - Unconditionally stable time-domain algorithm for solving full vector Maxwell's equations*, IEEE Trans. Microwave Theory Tech., 48 (2000), pp. 1743–1748.

[13] F. NERI, *Lie algebras and canonical integration*, University of Maryland, Dept. of Physics, preprint, (1987).

[14] D. PEACEMAN AND H. RACHFORD, JR., *The numerical solution of parabolic and elliptic differential equations*, J. Soc. Indust. Appl. Math., 3 (1955), pp. 28–41.

[15] V. PEREYRA, *Accelerating the convergence of discretization algorothm*, SIAM J. Numer. Anal., 4 (1967), pp. 508–532.

[16] L. RICHARDSON, *The deferred approach to the limit*, Phil. Trans. A, 226 (1927), pp. 299–349.

[17] G. STRANG, *On construction and comparison of difference schemes*, SIAM J. Numer. Anal., 5 (1968), pp. 506–516.

[18] M. SUZUKI, *General theory of fractal path integral with applications to many-body theories and statistical physics*, J. Math. Phys., 32 (1991), pp. 400–407.

[19] A. TAFLOVE AND S. HAGNESS, *Computational Electrodynamics: The Finite-Difference Time-Domain Method*, Arctech House, Boston, MA, 2nd ed., 2000.

[20] V. VARADRAJAN, *Lie groups, Lie algebras and their representation*, Applied Mathematics and Mathematical Computation, Prentice Halll, Englewood Cliffs, 1973.

[21] K. Yee, *Numerical solution of initial boundary value problems involving Maxwell's equations in isotropic media*, IEEE. Trans. Antennas Propagat., Ap-14 (1966), pp. 302–307.

[22] H. Yoshida, *Construction of higher order symplectic integrators*, Phys. Lett. A, 150 (1990), pp. 262–268.

[23] F. Zheng, Z. Chen, and J. Zhang, *A finite–difference time–domain method without the courant stability conditions*, IEEE Microwave Guided Wave Lett., 9 (1999), pp. 441–443.

[24] ——, *Toward the development of a three–dimensional unconditionally stable finite–difference time–domain method*, IEEE Trans. Microwave Theory Tech., 48 (2000), pp. 1550–1558.